



Journal of Catalysis Vol. 262, No. 1, 2009

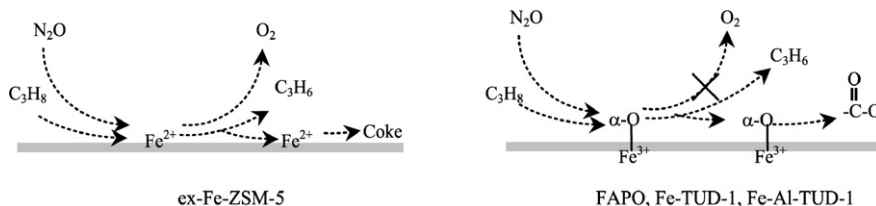
## Contents

## REGULAR ARTICLES

FAPO and Fe-TUD-1: Promising catalysts for N<sub>2</sub>O mediated selective oxidation of propane?

pp 1–8

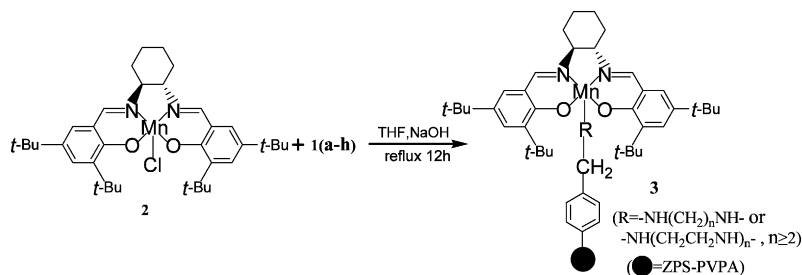
Wei Wei, Jacob A. Moulijn, Guido Mul\*

N<sub>2</sub>O mediated propane oxidation pathway over reduced (left) and oxidized (right) Fe-sites in micro- and mesoporous materials.

## Synthesis of a new type of immobilized chiral salen Mn(III) complex as effective catalysts for asymmetric epoxidation of unfunctionalized olefins

pp 9–17

Biwei Gong, Xiangkai Fu\*, Junxian Chen, Yuedong Li, Xiaochuan Zou, Xiaobo Tu, Pingping Ding, Liping Ma

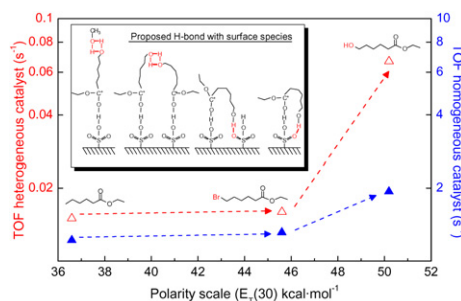


New types of ZAMPS-PVPA-immobilized chiral salen Mn(III) complexes were synthesized and used as catalysts in the asymmetric epoxidation of unfunctionalized olefins.

## Polarity of the acid chain of esters and transesterification activity of acid catalysts

pp 18–26

D. Martín Alonso, M. López Granados\*, R. Mariscal, A. Douhal

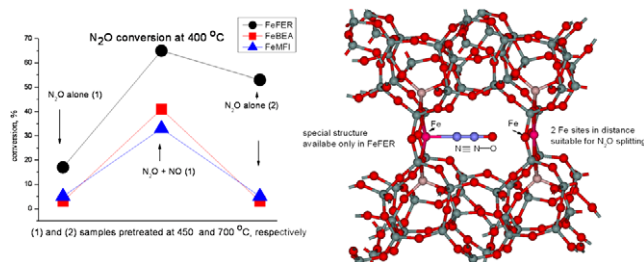


Ester methanolysis reaction rate on solid acid catalysts is accelerated when the ester has a polar group with capacity to form H-bonds with surface species whereas is rather unaffected when the polar group cannot establish the H-bonds.

## Role of the Fe-zeolite structure and iron state in the N<sub>2</sub>O decomposition: Comparison of Fe-FER, Fe-BEA, and Fe-MFI catalysts

pp 27–34

K. Jířša, J. Nováková, M. Schwarze, A. Vondrová, S. Sklenák, Z. Sobalík\*

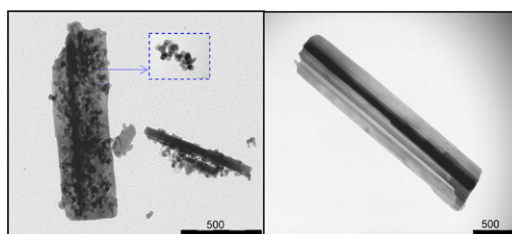


DFT model of the proposed active site for the N<sub>2</sub>O decomposition over Fe-FER. This local structure with unique spatial properties could provide for N<sub>2</sub>O splitting by mutual action of two adjacent iron cations in Fe-FER.

## Selective propane oxidation over MoVSbO catalysts. On the preparation, characterization and catalytic behavior of M1 phase

pp 35–43

Francisco Ivars, Benjamín Solsona, Enrique Rodríguez-Castellón, José M. López Nieto\*

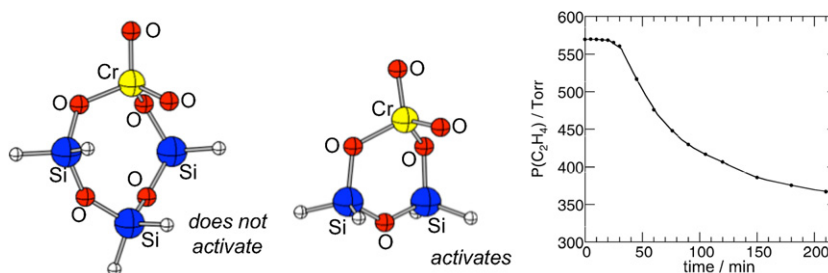


The preparation method of M1-pure containing MoVSbO catalysts strongly influences both the surface composition and the number of effective sites of M1 crystals, which determines their catalytic behavior in the propane selective oxidation to acrylic acid.

## Evidence for a chromasiloxane ring size effect in Phillips (Cr/SiO<sub>2</sub>) polymerization catalysts

pp 44–56

Cori A. Demmelmaier, Rosemary E. White, Jeroen A. van Bokhoven, Susannah L. Scott \*

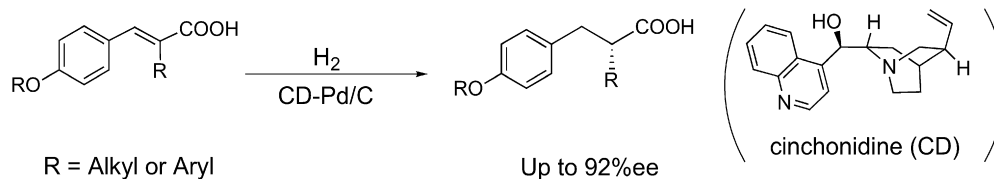


XANES suggests that the uniform chromate sites formed by grafting chromyl chloride onto silicas pretreated at low and high temperatures differ in the size of their chromasiloxane rings, and in the ability of these sites to initiate ethylene polymerization.

## Structural requirements for substrate in highly enantioselective hydrogenation over the cinchonidine-modified Pd/C

pp 57–64

Takashi Sugimura\*, Takayuki Uchida, Junya Watanabe, Takeshi Kubota, Yasuaki Okamoto, Tomonori Misaki, Tadashi Okuyama

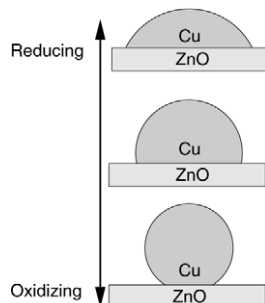


Relationship between substrate structure and enantioselectivity was studied with 42 different (*E*)- $\alpha,\beta$ -disubstituted acrylic acids for the hydrogenation over cinchonidine-modified Pd/C. The high ee was achieved with the  $\beta$ -*p*-alkoxyphenyl analogues.

**Transient behavior of Cu/ZnO-based methanol synthesis catalysts**

pp 65–72

Peter C.K. Vesborg, Ib Chorkendorff, Ida Knudsen, Olivier Balmes, Jesper Nerlov, Alfons M. Molenbroek, Bjerne S. Clausen, Stig Helveg \*

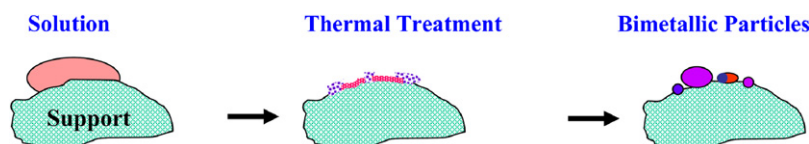


The transient production of methanol over a Cu/ZnO-based catalyst depends on the pretreatment gas conditions and is explained by observations of the gas-dependent shape of Cu nanocrystals supported on ZnO.

**In situ preparation of Ni–Cu/TiO<sub>2</sub> bimetallic catalysts**

pp 73–82

P. Li, J. Liu, N. Nag, P.A. Crozier\*

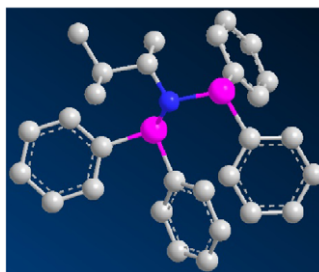


A nanoscale view of the processes that may occur when co-impregnation techniques are employed in the preparation of bimetallic catalysts. Salt solution interacts with support and thermal processing results in decomposition of precursor. Reduction leads to nucleation and growth of bimetallic particles which may vary in composition.

**Chromium catalyzed tetramerization of ethylene in a continuous tube reactor—Proof of concept and kinetic aspects**

pp 83–91

Sven Kuhlmann, Caspar Paetz, Christian Hägele, Kevin Blann, Richard Walsh, John T. Dixon, Judith Scholz, Marco Haumann, Peter Wasserscheid\*

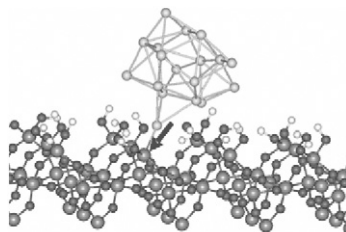


Our paper reports the first continuous tri- and tetramerization of ethylene in a plug flow tubular reactor utilizing a catalyst comprising Cr(acac)<sub>3</sub>, 1,2-dimethylpropyl-bis(diphenylphosphino)amine ligand and the aluminum-based activator MMAO-3A. Ligand of the catalytic system for the continuous selective tri- and tetramerization of ethylene.

**Thermal stability and catalytic activity of gold nanoparticles supported on silica**

pp 92–101

Gabriel M. Veith\*, Andrew R. Lupini, Sergey Rashkeev, Stephen J. Pennycook, David R. Mullins, Viviane Schwartz, Craig A. Bridges, Nancy J. Dudney

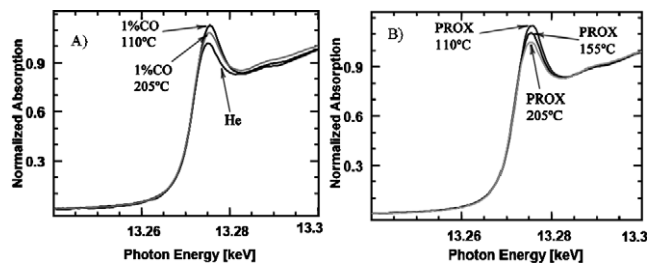


SiO<sub>2</sub> supported gold nanoparticles are shown to be significantly more thermally stable in air at high temperatures (500 °C) than prototypical Au/TiO<sub>2</sub> catalysts. While the Au/SiO<sub>2</sub> catalysts are less active for CO oxidation than the Au/TiO<sub>2</sub> catalysts, they can be regenerated far more easily, allowing the activity of a catalyst to be fully recovered after deactivation.

### **In situ EXAFS and FTIR studies of the promotion behavior of Pt–Nb<sub>2</sub>O<sub>5</sub>/Al<sub>2</sub>O<sub>3</sub> catalysts during the preferential oxidation of CO**

pp 102–110

S. Guerrero, J.T. Miller, A.J. Kropf, E.E. Wolf\*

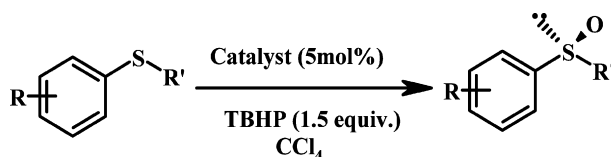


XANES results of the Pt/Nb/Al<sub>2</sub>O<sub>3</sub> catalysts under CO (A) and PROX (B) reaction conditions suggest that their surface is complex, containing reduced and oxidized Pt, which is modified by NbO<sub>x</sub> species either surrounding the Pt crystallites or decorating them.

### **Synthesis of chiral sulfoxides by enantioselective sulfide oxidation and subsequent oxidative kinetic resolution using immobilized Ti–binol complex**

pp 111–118

Suman Sahoo, Pradeep Kumar, F. Lefebvre, S.B. Halligudi\*

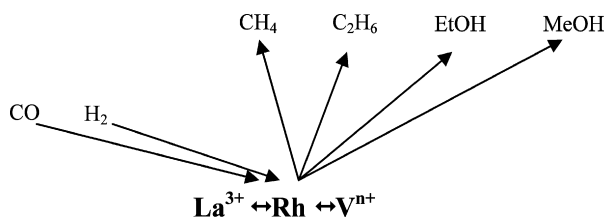


A supported ionic liquid strategy has been applied for the immobilization of chiral Ti–binol complex onto mesoporous silica. This catalyst system was utilized in the synthesis of chiral sulfoxides. This catalyst can be recovered and recycled for eight times without any loss of activity and enantioselectivity.

### **CO hydrogenation on lanthana and vanadia doubly promoted Rh/SiO<sub>2</sub> catalysts**

pp 119–126

Jia Gao, Xunhua Mo, Andrew Chang-Yin Chien, Walter Torres, James G. Goodwin Jr. \*

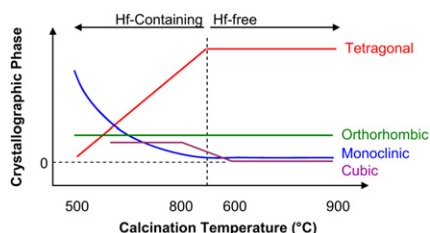


The combined promoting effect of La and V oxides for ethanol formation during CO hydrogenation on silica-supported Rh catalysts is reported.

### **Overcoming the deleterious effect of hafnium in tungsten–zirconia catalysts: The use of doping and thermal treatments**

pp 127–133

David Simon, Bradley Taylor\*

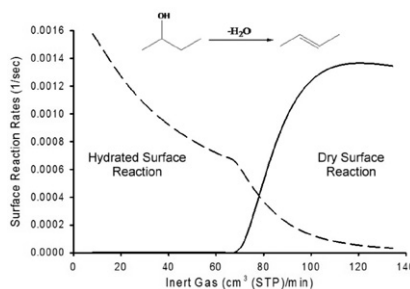


Hafnium impurities require high calcination temperatures to produce catalytically active tetragonal zirconia. The addition of aluminum also reduces the detrimental effect of hafnium on crystal structure.

**Dehydration of butanol to butene over solid acid catalysts in high water environments**

pp 134–143

Ryan M. West, Drew J. Braden, James A. Dumesic\*

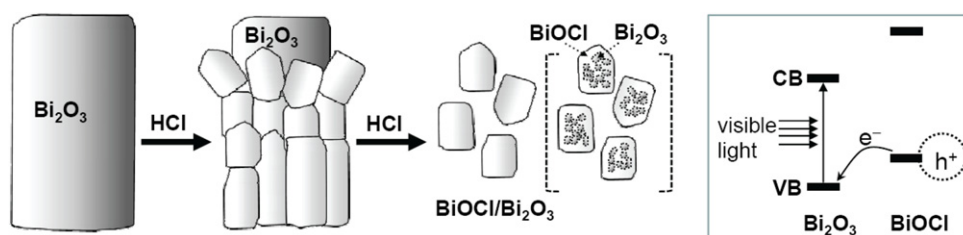


A kinetic model is able to seamlessly predict the transition from a mixed vapor–liquid regime to a completely vaporized regime for butane dehydration in the presence of water.

**Heterojunctioned BiOCl/Bi<sub>2</sub>O<sub>3</sub>, a new visible light photocatalyst**

pp 144–149

Seung Yong Chai, Yong Joo Kim, Myong Hak Jung, Ashok Kumar Chakraborty, Dongwoon Jung, Wan In Lee\*

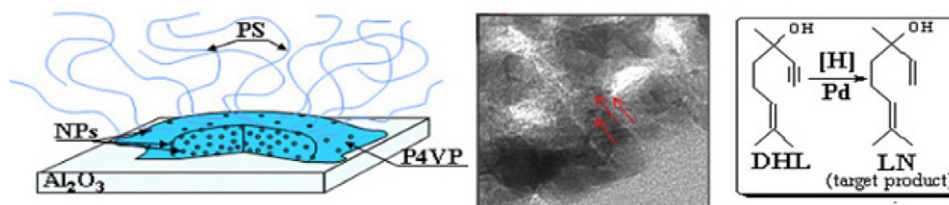


In the present study, we report that the heterojunction structure between BiOCl and Bi<sub>2</sub>O<sub>3</sub> can be an efficient photocatalyst under visible light irradiation, even though individual BiOCl and Bi<sub>2</sub>O<sub>3</sub> show very low photocatalytic efficiency.

**Influence of heterogenization on catalytic behavior of mono- and bimetallic nanoparticles formed in poly(styrene)-*block*-poly(4-vinylpyridine) micelles**

pp 150–158

Esther M. Sulman, Valentina G. Matveeva, Mikhail G. Sulman, Galina N. Demidenko, Pyotr M. Valetsky, Barry Stein, Tom Mates, Lyudmila M. Bronstein\*

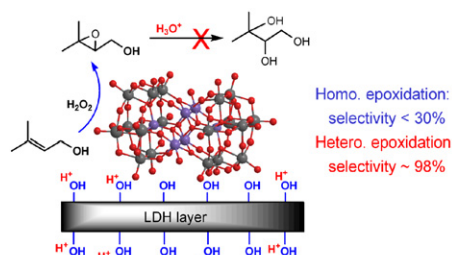


Influence of heterogenization on catalytic properties of block copolymer micellar catalysts derived from polystyrene-*block*-poly-4-vinylpyridine and containing Pd monometallic and bimetallic PdAu, PdPt, and PdZn nanoparticles have been studied in selective hydrogenation of the triple bond of 3,7-dimethyloctaen-6-yne-1-ol-3 (dehydrolinalool).

**Epoxidation of allylic alcohols on self-assembled polyoxometalates hosted in layered double hydroxides with aqueous H<sub>2</sub>O<sub>2</sub> as oxidant**

pp 159–168

Peng Liu, Changhao Wang, Can Li\*

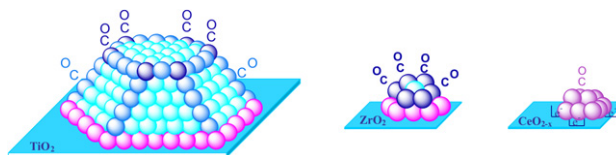


Layered double hydroxides (LDH)-hosted polyoxometalate (POM) catalysts show much higher epoxide selectivity than the corresponding homogeneous POM catalysts, which can be attributed to the beneficial effect of basic LDH host on the suppression of the acid-catalyzed epoxide hydrolysis.

### New insight on the nature of catalytically active gold sites: Quantitative CO chemisorption data and analysis of FTIR spectra of adsorbed CO and of isotopic mixtures

pp 169–176

Anna Chiorino, Maela Manzoli, Federica Menegazzo, Michela Signoretto, Floriana Vindigni, Francesco Pinna, Flora Bocuzzi\*



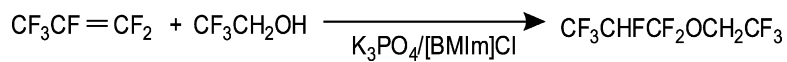
$^{12}\text{CO}$  and  $^{12}\text{CO}$ – $^{13}\text{CO}$  FTIR absorption spectra combined with quantitative chemisorption data pointed out the relationship between the nanostructure and the physical/chemical properties of Au catalysts supported on group IV oxides. On Au/TiO<sub>2</sub>, the CO adsorbing sites are mutually interacting edge and corner sites of Au metallic particles, while on Au/ZrO<sub>2</sub>, the adsorbing sites are mutually interacting corners of non metallic Au nanoclusters. Finally, almost isolated and negatively charged Au nanoclusters have been evidenced on CeO<sub>2</sub>. The differences between the absorption coefficients of CO on Au sites have been discussed. On all samples, by contacting CO– $^{18}\text{O}_2$  at 90 K, only C<sup>16</sup>O<sup>18</sup>O is produced, suggesting that only the gold sites are involved in the activation of both molecules.

#### RESEARCH NOTE

### Ionic liquid-assisted hydroalkoxylation of hexafluoropropene with 2,2,2-trifluoroethanol: A mechanistic consideration

pp 177–180

Je Eun Kang, Je Seung Lee, Dong Sub Kim, Sang Deuk Lee, Hyunjoon Lee, Hoon Sik Kim\*, Minserk Cheong\*



CF<sub>3</sub>CHFCF<sub>2</sub>OCH<sub>2</sub>CF<sub>3</sub> was obtained in high yield and selectivity from the hydroalkoxylation reaction of hexafluoropropene with 2,2,2-trifluoroethanol in the presence of a catalytic system consisting of K<sub>3</sub>PO<sub>4</sub> and [BMIm]Cl.